IEEE Access
Multidisciplinary : Rapid Review : Open Access Journal

Received September 17, 2020, accepted September 24, 2020, date of publication September 28, 2020, date of current version October 9, 2020.

Digital Object Identifier 10.1109/ACCESS.2020.3027354

Energy-Saving Trajectory Tracking Control of a Multi-Pump Multi-Actuator Hydraulic System

RUIKAI BAO[1], QINGFENG WANG[1], (Member, IEEE), AND TAO WANG[2], (Member, IEEE)
[1]State Key Laboratory of Fluid Power and Mechatronic System, Zhejiang University, Hangzhou 310027, China
[2]Ocean College, Zhejiang University, Hangzhou 310027, China

Corresponding author: Tao Wang (twang001@126.com)

This work was supported in part by the National Natural Science Foundation of China under Grant 51475414 and Grant 51875504, and in part by the Foundation for Innovative Research Groups of the National Natural Science Foundation of China under Grant 51821093.

ABSTRACT With the increasing application of automated hydraulic excavators, the demand for high-level control performance and significant energy saving schemes becomes stronger. The traditional hydraulic excavators with single-pump power source have amounts of coupling loss on throttling valves due to multi-actuator effect. Moreover, their operability is usually influenced by the load varying in a large range. This paper proposes a multi-pump system with on-off valve matrix to eliminate the coupling loss by dividing the system into several single-pump single-actuator subsystems. A pump/valve coordinate control strategy with multiple working modes is developed to adapt the load variation. First, mathematical modeling including mechanical part and hydraulic part is carried out based on dynamic analysis. Second, a three-level coordinated control scheme is proposed: 1) The motion tracking level utilizes backstepping control technique with load observation to obtain the desired hydraulic force; 2) The working mode switching level configures the pump and valve control mode to maximize energy saving according to load condition; 3) The force control level utilizes control technique to guarantee the stability and dynamic performance. Finally, comparative experimental results are presented to show the good control performance and significant energy saving achieved by the proposed multi-pump multi-actuator system as well as the control strategy.

INDEX TERMS Energy saving, multi-pump multi-actuator system, pump/valve coordinate control, mode switch, load observation.

I. INTRODUCTION

Energy crisis and environmental pollution become more and more serious challenges that we have to face. Hydraulic systems transmit a large amount energy with remarkable low efficiency. Therefore, the energy saving technology of hydraulic systems have drawn great research interests in recent years [1], [2].

The energy saving for hydraulic systems with trajectory tracking control has two typical methods. The first approach is to control the displacements of pumps to adapt load requirement. The hydro-mechanical load sensing (HMLS) system is widely used by controlling the pump displacement to make the pump pressure to match the highest load actuator [3]. However, this system is prone to slow response, low damping and oscillation. In addition, the HMLS system needs compensation valves to control the flow for different actuators so that there still exists throttling loss. The electronic load sensing (ELS) system can be used to improve the control performance, but it is no help for energy saving [4]. The electric flow matching (EFM) system controls the pump displacement according to required flow rates so as to increase responding speed and avoid oscillation tendency [5], [6]. It also can reduce pressure threshold in comparison with LS system. However, the flow mismatch between the pumps and the valves may lead to pressure impact and power loss. Direct pump control is to control the movement of actuators without valves, but its dynamic response is generally slower than throttling control, for the valves have inherent small inertia [7], [8]. The second approach is to control the proportional valves to meet the load demand. The meter-in and meter-out (MIMO) system [9], which decouples

The associate editor coordinating the review of this manuscript and approving it for publication was Javed Iqbal.

the traditional proportional directional valves (PDV), can increase control freedoms to realize pressure control and motion control at the same time. A programmable valve struct using pump/valve coordinate control is proposed and increases a parallel energy accumulator to tune flow [10]. This system synthesizes the control performance of valves and the high efficiency of pumps.

The above methods can achieve good energy saving for the single-actuator system, but not for the multi-actuator system because the traditional single-pump power source needs to match the highest load of multiple actuators. For other actuators with lower loads, it is inefficient because the proportional valves create an amount of throttling loss to match the corresponding load. The multi-pump system with matrix circuit is proposed to solve the above hydraulic coupling problem [11]. The grouped hydraulic pressure concept is presented in multi-pump system [12]. However, they focus on the energy saving but little on the tracking performance. In our previous paper, a multi-pump multi-actuator system is designed to decouple the multiple actuators [13]. The multi-actuator system can be divided into several single-pump single-actuator subsystems to eliminate the coupling throttling loss.

Automated hydraulic excavators are a typical application object of the multi-pump multi-actuator hydraulic system. The wide load variation of the automated hydraulic excavators in operation is another research challenge. The load can be divided into resistive load and overrunning load based on the directions of the load and the actuator motion. For the excavators, the overrunning load is common as the resistive load. Unlike the resistive load, only the pump control cannot work at overrunning load condition. The valve control should be used to balance the overrunning load. A pump/valve coordinate control is proposed to realize speed control and low pressure of pump at the overrunning load [14], [15]. However, it has not taken the load switch into consideration. Types of working conditions are analyzed and different working modes are designed to reduce energy loss [16]. The load is calculated by the measured pressure of the actuator and the mode switch based on calculated load will lead to transient process. The mode should be avoided switching frequently [17]–[20]. Besides, there are many control strategies are adopted to realize high-level trajectory tracking, such as slide control [21]–[24], adaptive control [25], ARC [10], [26], NN control [27], [28], learning-based optimal control [29], fuzzy control [30]–[32] and decentralized event-triggered control [33].

In this paper, we proposed a three-level control strategy for a multi-pump multi-actuator electro-hydraulic system. The contributions of this paper are reinterpreted in the revised introduction and given as follows.

1) In order to eliminate the coupling throttling loss, a multi-pump multi-actuator hydraulic system is proposed which can decouple the multiple-actuator effect.

2) A three-level pump/valve coordinate control strategy is proposed to adapt the load variation over a wide range in operation. The motion tracking level utilizes backstepping control technique with load observation to obtain the desired hydraulic force. The working mode level switching level configures the pump and valve control mode to maximize energy saving according to load condition. The force control level is to guarantee the stability and dynamic performance.

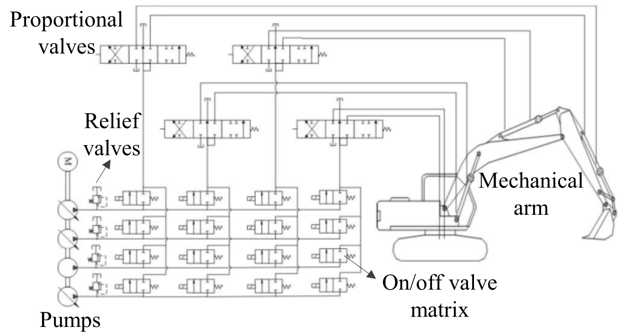

FIGURE 1. Schematic of proposed hydraulic system applied to an excavator.

The rest of this paper is organized as follows. Section II presents the model of the system. Section III presents the design of the controller. Section IV presents the cases study on the multi-pump multi-actuator experimental platform, and Section V draws the conclusion.

II. SYSTEM MODELING

A. SYSTEM SCHEME

The traditional single-pump multi-actuator system has an amount of coupling throttling loss because the pump pressure should adapt the actuator with the highest load. In order to reduce the coupling throttling loss, the concept of a multi-pump multi-actuator hydraulic system with on-off valve matrix is developed.

Figure.1 shows the simplified schematic of the proposed hydraulic system applied to an excavator. It mainly consists of multiple pumps, multiple actuators, mechanical arm, proportional valves and on-off valve matrix. The on-off valve matrix contains $n \times n$ pilot cartridge valves where n is the number of the actuators. When only the on-off valves on the diagonal line are open, the multi-actuator system can be divided into several single-pump single-actuator subsystems. It can cancel the coupling throttling loss and reduce the control complexity. This paper focuses on the motion control and energy saving of the decoupled system.

B. MECHANICAL ARM MODELING

The mechanical arm of excavator can be simplified to a three-degree-freedom linkage mechanism. The dynamic equation of mechanical arm is given as follow

$$M(\theta)\ddot{\theta} = \tau - c(\theta, \dot{\theta}) - g(\theta) - J_a^T(\theta)F_{tip} \tag{1}$$

where $M(\theta) \in \Re^{3\times 3}$ is the mass matrix, $\theta \in \Re^3, \dot{\theta} \in \Re^3, \ddot{\theta} \in \Re^3$ are the joint angle vector, angle velocity vector and angular acceleration vector, $\tau \in \Re^3$ is the driving torque vector, $c(\theta, \dot{\theta}) \in \Re^3$ is the sum of the coriolis force and centripetal force vector, $g(\theta) \in \Re^3$ is the gravity force vector, $J_a \in \Re^{3\times 3}$ is the jacobian matrix, $F_{tip} \in \Re^3$ is the lumped external load. The mass matrix $M(\theta)$ and gravity force vector

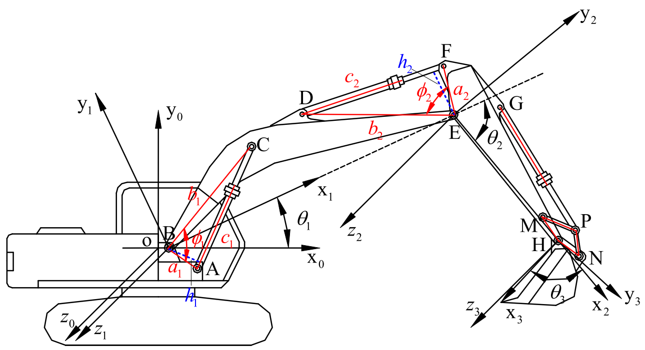

FIGURE 2. Schematic of an excavator with concerned coordinates.

$g(\theta)$ can be calculated in closed form based on the model parameters.

As shown in Figure 2, the driving mappings for boom and arm can be expressed as

$$\phi_i = \mathrm{acos}(\frac{a_i^2 + b_i^2 - (c_i + l_i)^2}{2a_i b_i}) \tag{2}$$

where ϕ_i is the angle of triangle corresponding to hydraulic cylinder of joint i, $i = 1$ and $i = 2$ stand for boom and arm respectively, a_i, b_i are constant edges length of driving triangle, c_i is the edges length of hydraulic cylinder when the cylinder extension l_i is zero.

The partial derivate of cylinder extension to triangle angle can be taken as

$$h_i = \frac{\partial l_i}{\partial \phi_i} = \frac{a_i b_i \sin(\phi_i)}{c_i + l_i} \tag{3}$$

where h_i stands for the moment arm of the hydraulic force where i is equal to 1 or 2.

The driving mapping between of pressure and driving torque can be calculated as

$$\begin{aligned} \tau_i &= w_i F_{q,i} h_i, \begin{cases} w_i = 1, i = 1 \\ w_i = -1, i = 2 \end{cases} \\ F_{q,i} &= F_i - B_i v_i - F_{f,i} \\ F_i &= p_{i,1} A_{i,1} - p_{i,2} A_{i,2} \end{aligned} \tag{4}$$

where w_i stands for the symbol from force mapping to torque, $F_{q,i}$ is the driving force to the mechanical arm, F_i is the hydraulic force, B_i is the friction coefficient, $F_{f,i}$ is the coulomb friction force, $p_{i,1}, p_{i,2}$ are the pressure of head side chamber and rod side chamber respectively, $A_{i,1}, A_{i,2}$ are the corresponding areas of actuator of joint i.

The joint angle just differs a constant with triangle angle can be given as

$$\theta_i = \phi_i + \phi_{0,i} \tag{5}$$

where $\phi_{0,i}$ is the constant value that is calculated according to the geometrical relationship.

The derivate of both side of equation (5) can be taken as

$$\begin{aligned} \dot{\theta}_i &= \dot{\phi}_i = J_{b,i} \dot{l}_i \\ \dot{l}_i &= J_{b,i}^{-1} \dot{\theta}_i = g_i(\dot{\theta}_i) \end{aligned} \tag{6}$$

where $g_i(\dot{\theta})$ is defined to simplify expression of jacobian matrix $J_{b,i}$.

The driving structure of buck increases a crank-rocker linkage with an extra angle mapping similarly. It is omitted due to page limit.

C. HYDRAULIC SYSTEM MODELING

The pressures of both chambers of cylinder can be given as

$$\begin{aligned} \dot{p}_{i,1} &= \frac{\beta_e}{V_{i,1}}(Q_{i,1} - \dot{l}_i A_{i,1}) \\ \dot{p}_{i,2} &= \frac{\beta_e}{V_{i,2}}(Q_{i,2} + \dot{l}_i A_{i,2}) \end{aligned} \tag{7}$$

where β_e is the effective bulk modulus, $V_{i,1}, V_{i,2}$ are the chambers volumes of cylinder i respectively, $Q_{i,1}, Q_{i,2}$ are the flow into the chambers respectively.

The volumes are changing with the cylinder extension, which can be described as

$$\begin{aligned} V_{i,1} &= V_{i,10} + A_{i,1} l_i \\ V_{i,1} &= V_{i,20} - A_{i,2} l_i \end{aligned} \tag{8}$$

where $V_{i,10}, V_{i,20}$ are the initial volumes of two chambers when cylinder extension is zero.

The flow mapping of pumps and proportional valves is very important that affects the control performance greatly. The pump flow mapping from the voltage input of amplified board to the output flow can be expressed as

$$Q_p = \begin{cases} k_p u_p + b_p - C_p(p_s - p_t), \\ \quad if\ (u > \dfrac{-b_q + C_p(p_s - p_t)}{k_q}) \\ 0, \quad other \end{cases} \tag{9}$$

where Q_p is output flow of pump, k_p is the gain and b_p is the offset, C_p is the leakage coefficient, p_s is pump pressure, p_t is the tank pressure, u_p is voltage input of pump amplified board.

The valve flow mapping from the voltage input of amplified board to the flow is strong nonlinear with differential pressure. A 3-layer neural network mapping structure is adapted as follow

$$Q_v = f_v(u_v, \Delta p) \tag{10}$$

where Q_v is the flow through the proportional valve, u_v is the control input of valve amplified board, Δp is the differential pressure of the valve.

Let us define the following state variables

$$\begin{aligned} [x_1, x_2, x_3, x_4, x_5] &= \left[\theta, \dot{\theta}, P_1, P_2, P_s\right] \\ P_1 &= \left[p_{1,1}, \ldots, p_{n,1}\right]^T \in \Re^n, \\ P_2 &= \left[p_{1,2}, \ldots, p_{n,2}\right]^T \in \Re^n \\ P_s &= \left[p_{1,s}, \ldots, p_{n,s}\right]^T \in \Re^n \end{aligned} \tag{11}$$

where n is 3 for excavator mechanical arm. And the above dynamic equations can be rewritten in the following state-space form

$$\begin{aligned} \dot{x}_1 &= x_2 \\ \dot{x}_2 &= M^{-1}(\tau - c(\theta, \dot{\theta}) - g(\theta) - J_a^T F_{tip}) \end{aligned}$$

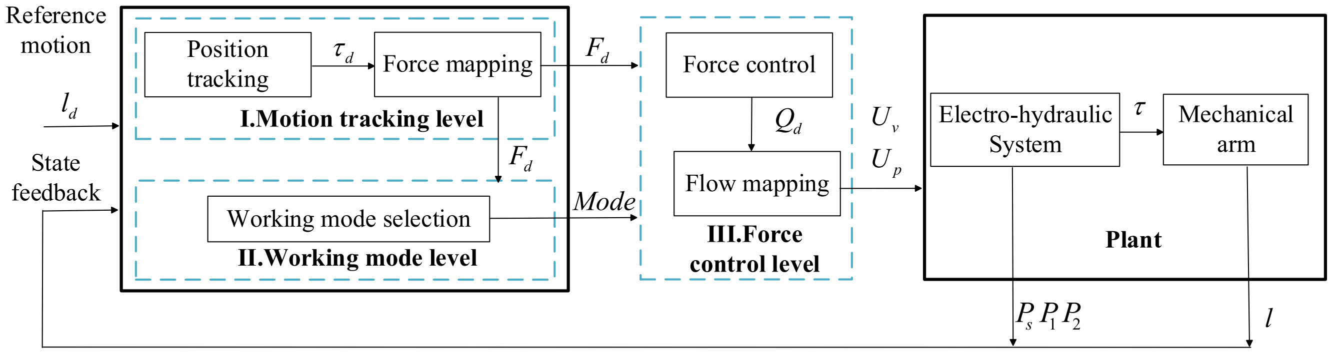

FIGURE 3. Control block diagram for the proposed hydraulic system.

$$
\begin{aligned}
\dot{x}_3 &= V_1^{-1}\beta_e(Q_1 - A_1 g(x_2)) \\
\dot{x}_4 &= V_2^{-1}\beta_e(Q_2 + A_2 g(x_2)) \\
\dot{x}_5 &= V_s^{-1}\beta_e(Q_p - Q_i), Q_i = \begin{cases} Q_{1,i}, & u_{v,i} > 0 \\ Q_{2,i}, & u_{v,i} < 0 \\ 0, & u_i = 0 \end{cases}
\end{aligned} \tag{12}
$$

where $V_1 = diag\{V_{1,1}, \ldots, V_{n,1}\}$, $V_2 = diag\{V_{1,2}, \ldots, V_{n,2}\}$

$$
\begin{aligned}
V_s &= diag\{V_{1,s}, ., V_{n,s}\}, A_1 = diag\{A_{1,1}, ., A_{n,1}\}, \\
A_2 &= diag\{A_{1,2}, ., A_{n,2}\} \\
g &= [g_1, g_2, g_3]^T, U_v = \left[u_{v,1}, \ldots, u_{v,n}\right]^T, \\
U_p &= \left[Q_{p,1}, \ldots, Q_{p,n}\right]^T
\end{aligned}
$$

$Q_a = [Q_1, \ldots, Q_n]^T$ and n is 3. Then pump control and valve control can be used to track the desired motion trajectory or pressure trajectory.

III. CONTROL STRATEGY

To sum up, the dynamics of the hydraulic system can be linearly parameterized as

$$
\begin{aligned}
\dot{x}_1 &= x_2 \\
\dot{x}_2 &= \alpha_1\tau - \alpha_1 c(x_1, x_2) - \alpha_1 g(x_1) - \alpha_2 \\
\dot{x}_3 &= \alpha_3 Q_1 - \alpha_4 g(x_2) \\
\dot{x}_4 &= \alpha_5 Q_2 + \alpha_6 g(x_2) \\
\dot{x}_5 &= \alpha_7(Q_p - Q_a)
\end{aligned} \tag{13}
$$

where $\alpha_1 = M^{-1}, \alpha_2 = M^{-1}J_a^T F_{tip}, \alpha_3 = V_1^{-1}\beta_e$
$\alpha_4 = V_1^{-1}\beta_e A_1, \alpha_5 = V_2^{-1}\beta_e, \alpha_6 = V_1^{-1}\beta_e A_2, \alpha_7 = V_s^{-1}\beta_e$.

Figure.3 presents the control block diagram of the proposed energy-saving hydraulic system. The controller is composed of three levels. The upper level is motion tracking level to attain the desired hydraulic force based on the load observation. The middle level is working mode level to determine working mode for pumps and proportional valves based on desired hydraulic force. The lower level is force control level to govern the actuators tracking performance.

A. MOTION TRACKING LEVEL

The mechanical arm can be considered as the load of the hydraulic actuators. The load consists of gravity load, digging force of bucket, friction and so on. Because the model of mechanical is known, the load including gravity load can be calculated by the measure states. The unknown time-varied load can be estimated by load observation. The lumped load can be divided into two parts as

$$
\begin{aligned}
\tau_l &= \tau_{l1} + \tau_{l2} \\
\tau_{l1} &= c(x_1, x_2) + g(x_1)
\end{aligned} \tag{14}
$$

where τ_{l1} is the calculated load by model and states, τ_{l2} is the unknown load.

The structure of load observation can be designed as

$$
\begin{aligned}
\dot{\hat{x}}_2 &= \hat{\alpha}_1\tau - \hat{\alpha}_1\tau_{l1} - \hat{\alpha}_1\dot{\hat{\tau}}_{l2} - k_{l1}(\hat{x}_2 - x_2) \\
\dot{\hat{\tau}}_{l2} &= -k_{l2}(\hat{x}_2 - x_2)
\end{aligned} \tag{15}
$$

where $\hat{x}_2$ is the estimated velocity, $\hat{\tau}_{l2}$ is the estimated unknown load. The load observation makes use of the model information and the velocity states besides the pressure. The lumped load is the sum of the calculated load and the observed load.

The desired driving torque can be calculated depending on the lumped load as feedforward compensate to realize motion tracking. The tracking error and derivate of error can be defined as follows

$$
\begin{aligned}
z_1 &= x - x_d \\
\dot{z}_1 &= \dot{x} - \dot{x}_d = z_2 \\
\dot{z}_2 &= \alpha_1(\tau - \tau_l) - \ddot{x}_d
\end{aligned} \tag{16}
$$

where z_1 is the tracking error and z_2 is the velocity error.

Then the desired torque can be designed as follows

$$
\begin{aligned}
\tau_d &= \tau_{da} + \tau_{ds} \\
\tau_{da} &= \hat{\tau}_l + \ddot{x}_{d,i}/\hat{\alpha}_1 \\
\tau_{ds} &= (-k_{s1}z_1 - k_{s2}z_2 - k_{s3}\int z_1 dt)/\hat{\alpha}_1
\end{aligned} \tag{17}
$$

where τ_{da} is the feedforward control based on the observed lumped load and desired angular acceleration, τ_{ds} is feedback control that consist state feedback and integral control to reduce tracking error, k_{s1}, k_{s2}, k_{s3} are the feedback gains.

Based on the equation (4), it is easy to attain the desired hydraulic force

$$
\begin{aligned}
F_d &= F_{da} + F_{ds} \\
F_{da} &= (wh)^{-1}\tau_{da} + Bv + F_f \\
F_{ds} &= (wh)^{-1}\tau_{ds}
\end{aligned} \tag{18}
$$

where F_{da} is the feedforward control and F_{ds} is feedback control.

TABLE 1. Working mode switching.

$\dot{l}_d$	F_{da}	$l-l_d$	Pump Mode	Valve Mode	Mode
$\dot{l}_d F_{da} \ge 0 \,\&\, \dot{l}_d \ne 0$		any	motion	max	PM
$\varepsilon < \dot{l}_d F_{da} \le 0 \,\&\, \dot{l}_d \ne 0$		any	pressure	motion	TM
$\dot{l}_d F_{da} \le \varepsilon \,\&\, \dot{l}_d \ne 0$		any	open-loop	motion	VM
0	any	$(-\infty,\delta)\cup(\delta,+\infty)$	open-loop	motion	R
0	any	$[-\delta,\delta]$	0	0	S

B. WORKING MODE LEVEL

Based on the desired hydraulic force and desired velocity, the working mode can be determined as TABEL I.

Mode PM: the direct pump control is used when the load is resistive for energy saving. The pump controls the motion of the actuator and the proportional valve opens maximumly to reduce the throttling loss.

Mode VM: the proportional valve control is used when the load is overrunning because the direct pump control cannot work to balance the load. The pump is controlled in open loop to make relief valve keep a little overflow. The enough high pressure can avoid the inlet chamber of actuator sucking air at the cost of extra energy consumption.

The mode PM and mode VM have different balanced states and control inputs. When the system switches quickly from mode VM to mode PM, the pump displacement cannot decrease at once but the proportional valve can open to maximum at once, which leads to speed overshoot. In order to guarantee the tracking precision, a transition mode TM is designed in switching from mode VM to mode PM.

Mode TM: the proportional valve controls the motion and the pump decreases the output pressure to adapt the load when the load varies from overrunning type to resistive type. The high dynamics of the valve can guarantee the tracking performance of the actuator when the load type changes. The key point is the design of the desired pump pressure for considering the dynamic of pump. It is reasonable to set the goal pressure as low as possible when near zero load. However, because of the big difference of the goal and current pump pressure, the desired pump pressure should be generated by a pressure planner to guarantee smoothness and satisfy the strict condition. The displacement of the pump will decrease to match the actuator and the proportional valve will open maximumly to reduce the throttling loss. The pressure planner can be design as

$$\min_{[P_r,Q_r]} \int_{t_1}^{t_2} P_r(t)Q_r(t)d\tau$$
$$s.t. \begin{cases} \dot{P}_r = V_s^{-1}\beta_e(Q_r - Q_d) \\ |\dot{Q}_s| \le \dot{Q}_{s,\max} \\ P_r(t_2) = P_d \end{cases} \tag{19}$$

where Q_d is the desired demand flow of actuator, $\dot{Q}_{s,\max}$ is the maximum displacement change rate of pump, P_d is preset goal pressure at time t_2, P_r is the desired pump pressure and Q_r is the desired flow of pump. Once the proportional is open maximumly or the time reaches t_2, the mode TM is finished and switching into PM mode.

Mode R is designed to realize precision location at the end point. Mode S is the stop mode nearest end point to avoid mode switching frequently of measure noise.

C. FORCE CONTROL LEVEL

Depending on the working mode and the desired hydraulic force, the force control level can be designed. The force error and derivate of force can be taken as follows

$$\begin{aligned} z_3 &= F - F_d \\ \dot{z}_3 &= \dot{F} - \dot{F}_d \\ &= (A_1\dot{P}_1 - A_2\dot{P}_2) - \dot{F}_d \\ &= A_1(\alpha_3 Q_1 - \alpha_4 g(x_2)) \\ &\quad - A_2(\alpha_5 Q_2 + \alpha_6 g(x_2)) - \dot{F}_d \end{aligned} \tag{20}$$

where z_3 is the error of the actual hydraulic force and the desired hydraulic force.

When then actuators are working on mode PM, the valves are open maximumly depending the motion direction

$$U_v = \begin{cases} U_{v\max}, & \dot{l}_d > 0 \\ -U_{v\max}, & \dot{l}_d < 0 \end{cases} \tag{21}$$

The pump pressure can be seen the same as the inlet chamber pressure of actuator when the valve open maximumly

$$x_5 \approx \begin{cases} x_3, & \dot{l}_d > 0 \\ x_4, & \dot{l}_d < 0 \end{cases} \tag{22}$$

The desired flow of pumps can be as designed as follows

$$\begin{aligned} Q_p &= Q_{pa} + Q_{ps} \\ Q_{pa} &= \begin{cases} A_1 g(x_{2d}) + A_1^{-1}(\hat{\alpha}_3^{-1} + \hat{\alpha}_7^{-1})^{-1}\dot{F}_d, U_v > 0 \\ -A_2 g(x_{2d}) - A_2^{-1}(\hat{\alpha}_5^{-1} + \hat{\alpha}_7^{-1})^{-1}\dot{F}_d, U_v < 0 \end{cases} \\ Q_{ps} &= \begin{cases} -k_{s4}A_1^{-1}(\hat{\alpha}_3^{-1} + \hat{\alpha}_7^{-1})^{-1} z_3, & U_v > 0 \\ -k_{s4}A_2^{-1}(\hat{\alpha}_3^{-1} + \hat{\alpha}_7^{-1})^{-1} z_3, & U_v > 0 \end{cases} \end{aligned} \tag{23}$$

where Q_p is the desired flow, Q_{pa} is feedforward control term consisting of two parts that one part is to stable the pressure with motion of the hydraulic cylinder and another part is to adapt the pressure to balance the load or making the hydraulic system to accelerate or deceleration. Q_{ps} is the feedback control term and k_{s4} is the feedback gain. Finally, the control input of pumps can be solved from the equation (9).

When the actuators are working on mode VM, the pump flow is a little bigger than the desired demand of actuator to make relief valve overflow. The equation (20) can be rewritten as

$$\begin{aligned} \dot{z}_3 &= Q_v - A_1\alpha_4 g(x_2) - A_2\alpha_6 g(x_2) - \dot{F}_d \\ Q_v &= A_1\alpha_3 f_v(u_v, \Delta P_1) - A_2\alpha_5 f_v(u_v, \Delta P_2) \end{aligned} \tag{24}$$

where $Q_v = A_1\alpha_3 f_v(u_v, \Delta P_1) - A_2\alpha_5 f_v(u_v, \Delta P_2)$ is the combined equivalent flow of both sides.

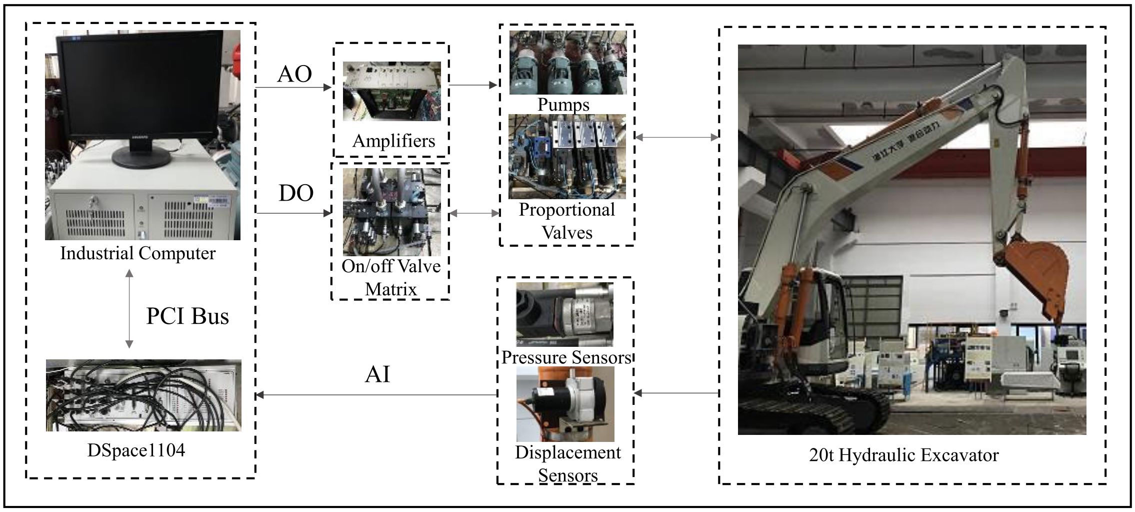

FIGURE 4. Experimental platform of multi-pump multi-actuator hydraulic system with on/off valve matrix.

Then desired flow of valves can be design as follows

$$\begin{aligned} Q_v &= Q_{va} + Q_{vs} \\ Q_{va} &= A_1\hat{\alpha}_4\hat{g}(x_{2d}) + A_2\hat{\alpha}_4\hat{g}(x_{2d}) + \dot{F}_d \\ Q_{vs} &= -k_{s5}z_3 \end{aligned} \tag{25}$$

where Q_{va} is the feedforward control term in which the first two items is the most important based on desired velocity. Q_{vs} is the feedback control term and k_{s5} is the feedback gain. Finally, the control input of valves can be solved from the equation (10).

When the actuators are working on mode TM, the valve control is the same as mode VM. The pump control is adapted to tracking the desired pump pressure. The tracking pressure error z_p can be defied as

$$z_p = P_s - P_r \tag{26}$$

The derivate of both side of equation (26) can be taken as

$$\dot{z}_p = \alpha_7(Q_p - Q_d) - \dot{P}_r \tag{27}$$

The desired flow of pump can be as designed as follows

$$\begin{aligned} Q_p &= Q_{pa} + Q_{ps} \\ Q_{pa} &= Q_d + \alpha_7^{-1}\dot{P}_r \\ Q_{ps} &= (-k_{s5}z_p - k_{s6}\int z_p dt)/\hat{\alpha}_7 \end{aligned} \tag{28}$$

where k_{s5}, k_{s6} are the feedback gains. Finally, the control input of pumps can be solved from the equation (9).

D. STABILITY ANALYSIS

The stability analysis of the proposed control strategy is by Lyapunov stability analysis. Firstly, we defined a positive scalar function as

$$V = \frac{1}{2}k_{s1}z_1^2 + \frac{1}{2}z_2^2 + \frac{1}{2}z_3^2 \tag{29}$$

The proof of stability for different modes is similar and the switching process is quick so that proof for mode PM is used to illustrate. The derivate of above positive function can be taken as follows

$$\begin{aligned} \dot{V} &= k_{s1}z_1\dot{z}_1 + z_2\dot{z}_2 + z_3\dot{z}_3 \\ &= k_{s1}z_1z_2 + z_2(\alpha_1(whz_3 - \frac{1}{\hat{\alpha}_1}k_{s1}z_1 \\ &\quad -\frac{1}{\hat{\alpha}_1}k_{s2}z_2 - \frac{1}{\hat{\alpha}_1}k_{s3}\int z_1 dt) + \xi_1) \\ &\quad +z_3(\frac{\hat{\alpha}_3^{-1} + \hat{\alpha}_7^{-1}}{\alpha_3^{-1} + \alpha_7^{-1}}(-\hat{\alpha}_1 whz_2 - k_{s4}z_3) + \xi_2) \\ &= -\frac{\alpha_1}{\hat{\alpha}_1}k_{s2}z_2^2 - \frac{\hat{\alpha}_3^{-1} + \hat{\alpha}_7^{-1}}{\alpha_3^{-1} + \alpha_7^{-1}}k_{s4}z_3^2 + \{-\frac{\tilde{\alpha}_1}{\hat{\alpha}_1}z_1z_2 \\ &\quad +(\alpha_1 - \frac{\hat{\alpha}_3^{-1} + \hat{\alpha}_7^{-1}}{\alpha_3^{-1} + \alpha_7^{-1}}\hat{\alpha}_1)whz_2z_3 + \xi_1z_2 + \xi_2z_3 \\ &\quad -\frac{\alpha_1}{\hat{\alpha}_1}k_{s3}z_2\int z_1 dt\} \\ &\le -\frac{\alpha_1}{\hat{\alpha}_1}k_{s2}z_2^2 - \frac{\hat{\alpha}_3^{-1} + \hat{\alpha}_7^{-1}}{\alpha_3^{-1} + \alpha_7^{-1}}k_{s4}z_3^2 + \zeta_{\max} \end{aligned} \tag{30}$$

where ξ_1, ξ_2 are uncertainties and disturbances respectively, $\zeta_{\max}$ is the lumped uncertainties and disturbances which is bounded. Reducing $\hat{\alpha}_1, \hat{\alpha}_3, \hat{\alpha}_7$ appropriately will improve the stability performance by ensuring $\dot{V}$ negative. The system is stable and the tracking errors are bounded by choice suitable control parameters.

IV. EXPERIMENT RESULTS

A. EXPERIMENT PLATFORM

The control system architecture of the multi-pump multi-actuator experimental platform is shown as Figure 4. The hardware consists of the proportional valves (REXROTH 4WRPH10), the on/off valve matrix, the variable displacement pumps (REXROTH A4VSO71 and A10VSO 45) and 20t excavator with mechanical arm. The key model parameters are marked in Figure 2 and Figure 5. The values of model parameters are shown in Table 2 which are obtained from

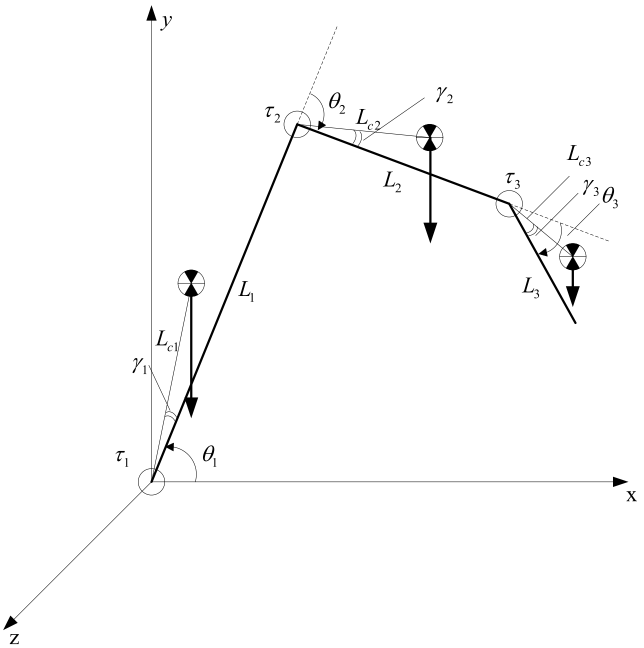

FIGURE 5. Simple structure of an excavate with key parameters.

practical 3D model. The sensors consist of pressure sensors and displacement sensors whose accuracies are ±1%FS and ±0.1% FS respectively. This work employs Matlab/Simulink as programming software to release controller. The controller hardware is DSpace1104 which supports Matlab/Simulink. The DSpace 1004 receives all the sensor signals and sends control signal to the amplifier boards. To verify the system performance, three cases of motion tracking experiments are implemented.

B. PRELIMINARY CONTROL PERFORMANCE

In general, PID controller has been widely used as a well-known control method. To show the advantages of the proposed algorithm, we added comparison experiments of arm under resistive load between the proposed algorithm and the PID controller.

B11: Proportional-integral-differential (PID) controller is used to tracking the desired trajectory. The PID gains are tunned as $k_p = 0.02$, $k_d = 0$, $k_i = 0.01$.

B12: The proposed controller of this paper is used to tracking the desired trajectory. The state feedback gains are given as $k_{s1} = -20$, $k_{s2} = -100$, $k_{s4} = k_{s5} = k_{s6} = -10$. The integral gains are given as $k_{s1} = k_{s7} = -2$.

The desired trajectories are shown in Figure 6 and the tracking performance comparisons are shown in Figure 7. The results show that the proposed controller (B12) can achieve better tracking performance than PID controller (B11).

C. CONTROL PERFORMANCE AND EFFICIENCY EVALUATION

1) CASE 1

The multi-pump system can decouple the system into several single-pump single-actuator subsystem to reduce the coupling throttling loss. The motion tracking of both boom and arm under resistive load is designed to verify the tracking performance and energy saving.

TABLE 2. Parameters of experimental platform.

Component	Parameter	Symbol	Value
Boom	Equivalent length	L_1(mm)	5610
	Length between gravity center and rotation center	L_{c1}(mm)	2905
	Angle of gravity center	γ_1(rad)	0.224
	Rotational inertia	$J_1(\mathrm{kg \cdot m^2})$	5426
	Mass	m_1(kg)	1996
	Area of head side chamber	$A_{1,1}(\mathrm{m^2})$	0.0213
	Area of rod side chamber	$A_{1,2}(\mathrm{m^2})$	0.0106
Arm	Equivalent length	L_2(mm)	2975
	Length between gravity center and rotation center	L_{c2}(mm)	1030
	Angle of gravity center	γ_2(rad)	0.182
	Rotational inertia	$J_2(\mathrm{kg \cdot m^2})$	1012
	Mass	m_2(kg)	872
	Area of head side chamber	$A_{2,1}(\mathrm{m^2})$	0.0133
	Area of rod side chamber	$A_{2,2}(\mathrm{m^2})$	0.0067

C11: the traditional single pump system is used. The highest load actuator is controlled by pump with the proportional valve opening maximumly. The lower load actuator is controlled by proportional valve.

C12: the proposed multi-pump system is used. The multiple actuators can be decoupled and are working on mode PM under resistive load.

The desired trajectories are shown in Figure 8 and the tracking performance comparisons are shown in Figure 9. The proposed multi-pump system in C12 achieves the same level of tracking precision as the single-pump system in C11.

The cylinders working pressures are shown in Figure 10. For the boom whose load higher, the proportional valve is opening maximumly to conserve energy and outlet pressure is at low levels and the inlet pressure is determined by the load. For the arm whose load lower, the valve opens small making the both pressure of inlet and outlet are higher in C11 than C12.

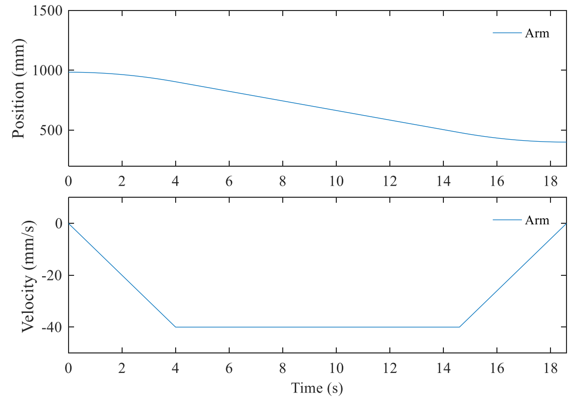

FIGURE 6. Desired trajectory of arm in controller comparison.

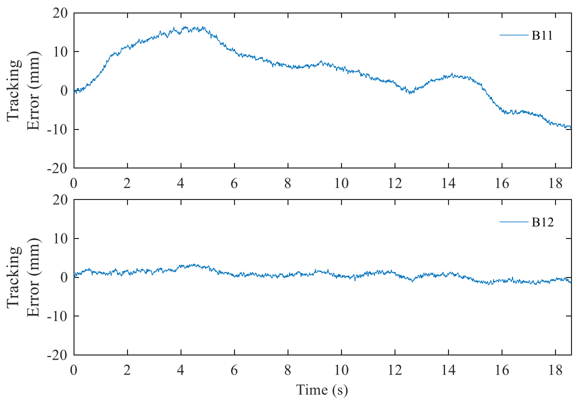

FIGURE 7. Tracking errors of arm in in controller comparison.

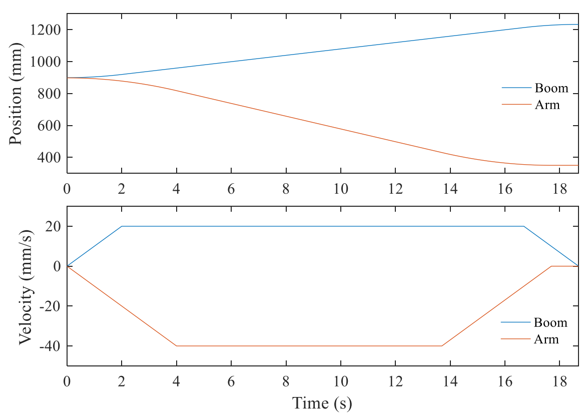

FIGURE 8. Desired trajectories of boom and arm in case 1.

The energy consumption is calculated by

$$P_{ow} = \int \sum_{i=1}^{n} p_{i,s} q_{i,s} dt \tag{31}$$

where P_{ow} is the energy consumption, $p_{i,s}$ and $q_{i,s}$ are the pressure and flow of pump i. $q_{i,s}$ is the mapping with control input of pump and pressure based on equation (9). $p_{i,s}$ can be obtained by pressure sensors.

The energy consumption comparisons of experiments are shown in Figure 11. It is apparent that C12 consumes far less energy compared to C11 and detailed results show about 26% less. The energy saving effort of the multi-pump system comes from the significant reduction of the coupling throttling loss.

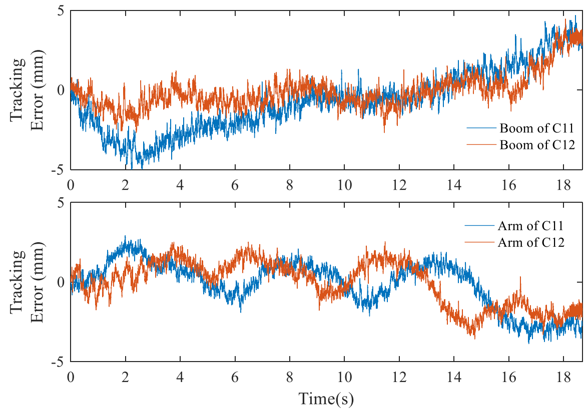

FIGURE 9. Tracking errors of boom and arm in case 1.

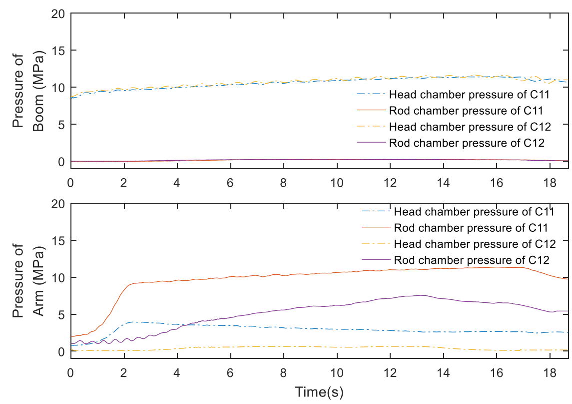

FIGURE 10. Pressures of two chambers of cylinders in case 1.

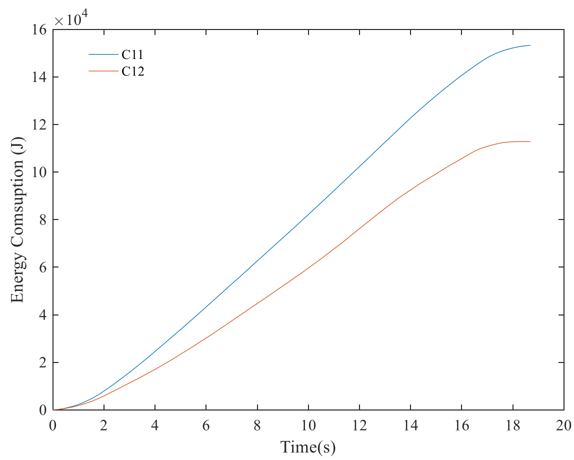

FIGURE 11. Comparative energy consumption in case 1.

2) CASE 2

The proposed control strategy can realize energy saving and high-level tracking under load variating over a wide range. The motion tracking of arm under different type load is designed to verify the effects.

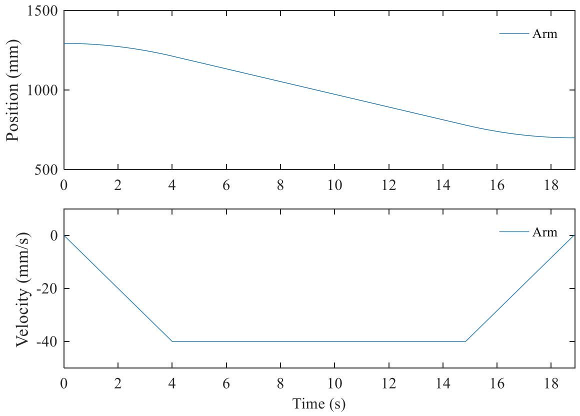

FIGURE 12. Desired trajectory of arm in case 2.

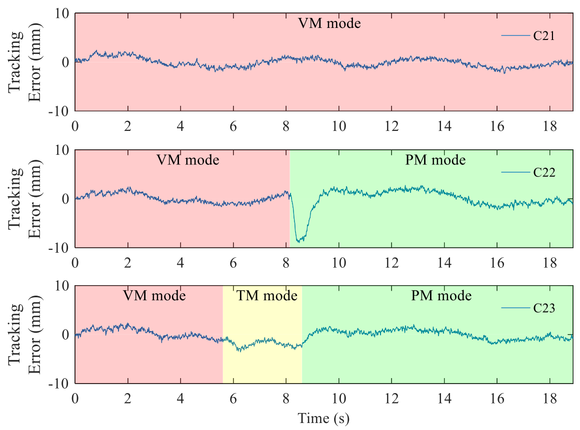

FIGURE 13. Tracking errors of arm in case 2.

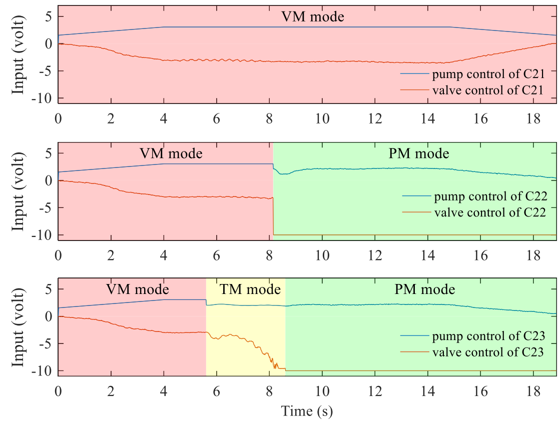

FIGURE 14. Control inputs of pump and valve of arm in case 2.

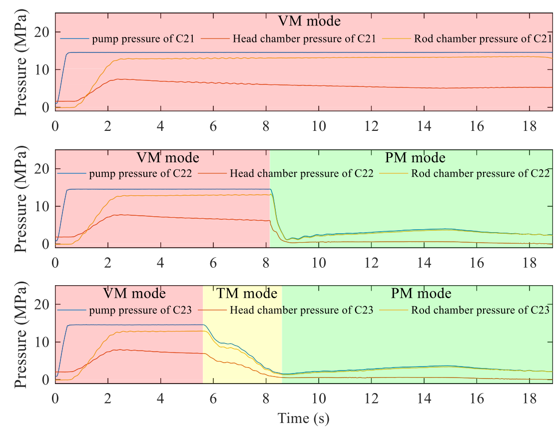

FIGURE 15. Pressures of two chambers of cylinder and pump of arm in case 2.

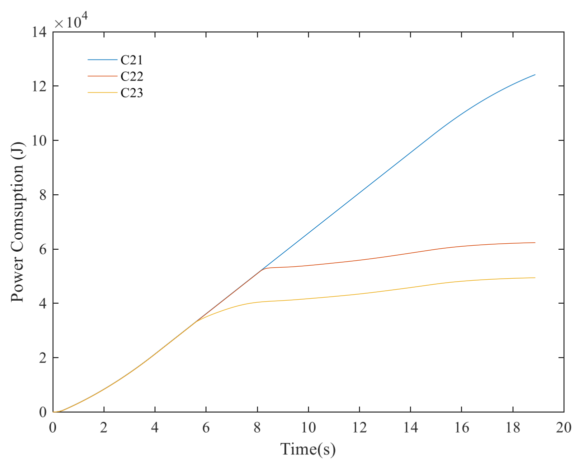

FIGURE 16. Comparative energy consumption of case 2.

C21: only the proportional valve control method under mode VM. This method can overcome the different type load because the valve control has the ability to balance load. The relief valve of pump keeps open to demand the load.

C22: the proposed pump/valve coordinate control without mode TM. The control inputs are jumping when mode switch instantaneously.

C23: the proposed pump/valve coordinate control with the mode TM to realize smooth transition.

The desired trajectory is shown in Figure 12 and the tracking performance comparisons are shown in Figure 13. The control inputs of pump and valve are shown in Figure 14. The proposed method in C23 achieves the same level tracking precision as the only valve control method in C21. The control method in C22 attains the worse tracking performance due to the control input jumping when mode switch directly. By using the mode TM as the transition between the mode VM and mode PM, the control inputs have enough time to changes smoothly so that the tracking error shooting is avoidable. Based on the load observation and backstepping control, the judge of the mode is more accurate and can avoid the pressure noise affecting the mode switch frequently.

The cylinders working pressures and pump pressure are shown in Figure 15. Because the C21 only uses mode VM, the both pressures of cylinder are higher than C22 and C23 when they are in mode PM. The pump pressures in C22 and C23 are lower than C21 in mode PM indicating a lot of throttling loss reduced. The C23 has mode TM before into mode PM so that the pressure can be controlled by pump to changing smoothly.

The energy consumption comparisons of experiments are shown in Figure 16. It is apparent that C22 and C23 consume far less energy compared to C21. The detailed results show

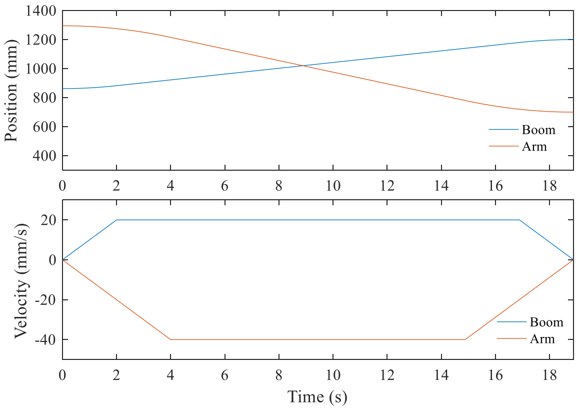

FIGURE 17. Desired trajectories of boom and arm in case 3.

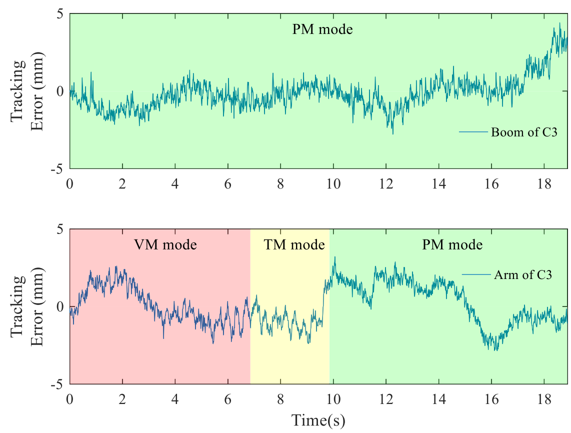

FIGURE 18. Tracking errors of boom and arm in case 3.

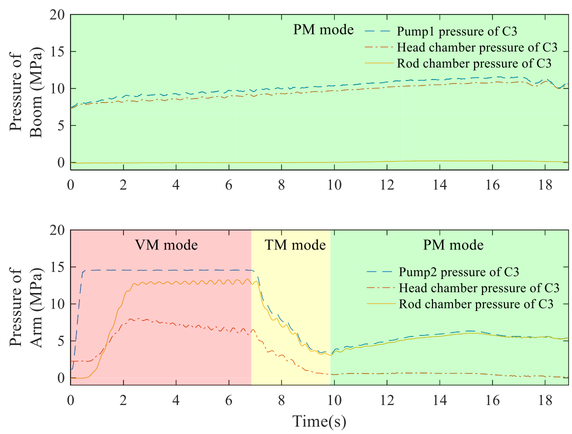

FIGURE 19. Pressures of two chambers of cylinder and pumps of boom and arm in case 3.

about 50% and 60% less respectively. The energy saving is significant by using the pump/valve coordinate control strategy with multiple working modes.

3) CASE 3

The motion tracking of both boom and arm under different type load is designed to verify the tracking performance and energy saving. The desired trajectory is shown in Figure 17 and the tracking performance are shown in Figure 18. The cylinders working pressures and pump pressure are shown in Figure 19. The proposed control strategy and multi-pump system can attain good tracking performance and energy saving for multiple actuators especially.

V. CONCLUSION

In this paper, a multi-pump multi-actuator hydraulic system is proposed that can decouple the multiple actuators into several single-pump single-actuator subsystems to eliminate the coupling throttling loss. Based on the mathematical modeling including mechanical part and hydraulic part, a three-level pump/valve coordinate control strategy is proposed to adapt the load variation over a wide range in operation. The comparative experiments are implemented and the results show that the proposed hydraulic system and control strategy can achieve good control performance and significant energy saving. In the future, the switching strategy of the on/off valve matrix and the dynamic performance optimization of the actuators in switching will be further studied.

REFERENCES

[1] T. Wang and Q. Wang, "An energy-saving pressure-compensated hydraulic system with electrical approach," *IEEE/ASME Trans. Mechatronics*, vol. 19, no. 2, pp. 570–578, Apr. 2014.

[2] T. Wang and Z. Zhou, "A compact hydrostatic-driven electric generator: Design, prototype, and experiment," *IEEE/ASME Trans. Mechatronics*, vol. 21, no. 3, pp. 1612–1619, Jun. 2016.

[3] M. Axin, B. Eriksson, and P. Krus, "A flexible working hydraulic system for mobile machines," *Int. J. Fluid Power*, vol. 17, no. 2, pp. 79–89, May 2016.

[4] R. H. Hansen, A. M. Iversen, M. S. Jensen, T. O. Andersen, and H. C. Pedersen, "Modeling and control of a teletruck using electronic load sensing," in *Proc. ASME 10th Biennial Conf. Eng. Syst. Design Anal.*, vol. 3, Jan. 2010, pp. 769–778.

[5] M. Cheng, J. Zhang, B. Xu, and R. Ding, "An electrohydraulic load sensing system based on flow/pressure switched control for mobile machinery," *ISA Trans.*, vol. 96, pp. 367–375, Jan. 2020.

[6] B. Xu, M. Cheng, H. Yang, J. Zhang, and C. Sun, "A hybrid displacement/pressure control scheme for an electrohydraulic flow matching system," *IEEE/ASME Trans. Mechatronics*, vol. 20, no. 6, pp. 2771–2782, Dec. 2015.

[7] B. Helian, Z. Chen, B. Yao, and C. Yang, "Designing an improved controller for a pump direct driven electro-hydraulic system using a nonlinear flow mapping," in *Proc. ASME/BATH Symp. Fluid Power Motion Control*, Oct. 2019, Art. no. V001T01A049.

[8] B. Helian, Z. Chen, B. Yao, Y. Yan, and C. Lee, "Adaptive robust control of a pump control hydraulic system," in *Proc. Dyn. Syst. Control Conf.*, Oct. 2017, Art. no. V001T15A004.

[9] B. Xu, R. Ding, J. Zhang, M. Cheng, and T. Sun, "Pump/valves coordinate control of the independent metering system for mobile machinery," *Autom. Construct.*, vol. 57, pp. 98–111, Sep. 2015.

[10] L. Lyu, Z. Chen, and B. Yao, "Development of pump and valves combined hydraulic system for both high tracking precision and high energy efficiency," *IEEE Trans. Ind. Electron.*, vol. 66, no. 9, pp. 7189–7198, Sep. 2019.

[11] H. Theissen, "Energy saving with a matrix circuit," in *Proc. Oelhydraulik Pneumatik*. 2009, pp. 340–343.

[12] L. Li, H. Huang, F. Zhao, and Z. Liu, "A coordinate method applied to partitioned energy-saving control for grouped hydraulic presses," *J. Manuf. Syst.*, vol. 41, pp. 10–102, Oct. 2016.

[13] R. Bao, T. Wang, and Q. Wang, "A multi-pump multi-actuator hydraulic system with on-off valve matrix for energy saving," in *Proc. IEEE/ASME Int. Conf. Adv. Intell. Mechatronics (AIM)*, Jul. 2019, pp. 1110–1115.

[14] M. Jin and Q. Wang, "Efficient pump and meter-out control for electrohydraulic system with time-varying negative load," *Proc. Inst. Mech. Eng. I, J. Syst. Control Eng.*, vol. 232, pp. 1170–1181, Oct. 2018.

[15] M. Jin and Q. Wang, "Energy-saving control for electro-hydraulic systems under time-varying negative loads," *Proc. Inst. Mech. Eng. I, J. Syst. Control Eng.*, vol. 232, pp. 608–621, May 2018.

[16] R. Ding, J. Zhang, B. Xu, M. Cheng, and M. Pan, "Energy efficiency improvement of heavy-load mobile hydraulic manipulator with electronically tunable operating modes," *Energy Convers. Manage.*, vol. 188, pp. 447–461, May 2019.

[17] L. Lyu, Z. Chen, and B. Yao, "Energy saving motion control of independent metering valves and pump combined hydraulic system," *IEEE/ASME Trans. Mechatronics*, vol. 24, no. 5, pp. 1909–1920, Oct. 2019.

[18] L. Lu and B. Yao, "Energy-saving adaptive robust control of a hydraulic manipulator using five cartridge valves with an accumulator," *IEEE Trans. Ind. Electron.*, vol. 61, no. 12, pp. 7046–7054, Dec. 2014.

[19] S. Liu and B. Yao, "Coordinate control of energy saving programmable valves," *IEEE Trans. Control Syst. Technol.*, vol. 16, no. 1, pp. 34–45, Jan. 2008.

[20] T. Wang, Y. Zhang, Z. Chen, and S. Zhu, "Parameter identification and model-based nonlinear robust control of fluidic soft bending actuators," *IEEE/ASME Trans. Mechatronics*, vol. 24, no. 3, pp. 1346–1355, Jun. 2019.

[21] J. Yao, W. Deng, and Z. Jiao, "Adaptive control of hydraulic actuators with LuGre model-based friction compensation," *IEEE Trans. Ind. Electron.*, vol. 62, no. 10, pp. 6469–6477, Oct. 2015.

[22] S. Mobayen, "Design of lmi-based sliding mode controller with an exponential policy for a class of underactuated systems," *Complexity*, vol. 21, no. 5, pp. 117–124, 2016.

[23] S. Mobayen and J. Ma, "Robust finite-time composite nonlinear feedback control for synchronization of uncertain chaotic systems with nonlinearity and time-delay," *Chaos, Solitons Fractals*, vol. 114, pp. 46–54, Sep. 2018.

[24] S. Mobayen and F. Tchier, "Nonsingular fast terminal sliding-mode stabilizer for a class of uncertain nonlinear systems based on disturbance observer," *Scientia Iranica*, vol. 24, no. 3, pp. 1410–1418, Jun. 2017.

[25] C. Guan and S. Pan, "Adaptive sliding mode control of electro-hydraulic system with nonlinear unknown parameters," *Control Eng. Pract.*, vol. 16, no. 11, pp. 1275–1284, 2008.

[26] Y. Li and Q. Wang, "Adaptive robust tracking control of a proportional pressure-reducing valve with dead zone and hysteresis," *Trans. Inst. Meas. Control*, vol. 40, no. 7, pp. 2151–2166, 2018.

[27] Y. Li and Q. Wang, "Adaptive neural finite-time trajectory tracking control of hydraulic excavators," *Proc. Inst. Mech. Eng. I, J. Syst. Control Eng.*, vol. 232, no. 7, pp. 909–925, 2018.

[28] L. Ma, X. Huo, X. Zhao, and Z. GD, "Observer-based adaptive neural tracking control for output-constrained switched mimo nonstrict-feedback nonlinear systems with unknown dead zone," *Nonlinear Dyn.*, vol. 99, no. 2, pp. 1019–1036, 2020.

[29] J. Zhang, Q. Wang, and T. Wang, "A learning-based optimal tracking controller for continuous linear systems with unknown dynamics: Theory and case study," *Meas. Control*, vol. 53, pp. 778–787, May 2020.

[30] Y. Chang, Y. Wang, A. Fe, and G. Zong, "Adaptive fuzzy output-feedback tracking control for switched stochastic pure-feedback nonlinear systems," *Int. J. Adapt. Control Signal Process.*, vol. 33, no. 10, pp. 1567–1582, 2019.

[31] Z.-M. Li, X.-H. Chang, and J. H. Park, "Quantized static output feedback fuzzy tracking control for discrete-time nonlinear networked systems with asynchronous event-triggered constraints," *IEEE Trans. Syst., Man, Cybern. Syst.*, early access, Aug. 15, 2019, doi: 10.1109/TSMC.2019.2931530.

[32] L. Ma, X. Huo, X. Zhao, and G. Zong, "Adaptive fuzzy tracking control for a class of uncertain switched nonlinear systems with multiple constraints: A small-gain approach," *Int. J. Fuzzy Syst.*, vol. 21, no. 8, pp. 2609–2624, 2019.

[33] J. Cai, R. Yu, B. Wang, C. Mei, and L. Shen, "Decentralized event-triggered control for interconnected systems with unknown disturbances," *J. Franklin Inst.-Eng. Appl. Math.*, vol. 357, no. 3, pp. 1494–1515, 2020.

RUIKAI BAO received the B.Eng. degree from the Nanjing University of Aeronautics and Astronautics, Nanjing, China, in 2015, where he is currently pursuing the Ph.D. degree in mechatronic control engineering. His research interests include motion control and energy saving.

QINGFENG WANG (Member, IEEE) received the M.Eng. and Ph.D. degrees in mechanical engineering from Zhejiang University, Hangzhou, China, in 1988 and 1994, respectively. In 1994, he became a Faculty Member with Zhejiang University, where he was promoted to a Professor, in 1999. He was the Director of the State Key Laboratory of Fluid Power Transmission and Control, Zhejiang University, from 2001 to 2005, and currently serves as the Director of the Institute of Mechatronic Control Engineering. His research interests include electro-hydraulic control components and systems, hybrid power systems and energy saving techniques for construction machinery, and system synthesis for mechatronic equipment.

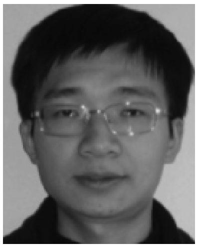

TAO WANG (Member, IEEE) was born in Shangrao, China, in 1987. He received the B.S. and Ph.D. degrees in mechanical engineering from Zhejiang University, China, in 2008 and 2013, respectively. From 2013 to 2016, he was a Lecturer with the College of Mechanical and Vehicle Engineering, Hunan University, China. He is currently an Associate Professor with the Ocean College, Zhejiang University. He has contributed over 30 academic publications and holds over ten patents. His research interests include marine mechatronic control, bionic soft robotics, and intelligent sensing. He is an Associate Editor of IEEE Access journal.